Temporal rates of major explosions and paroxysms at Stromboli: data and statistical models

Augusto Neri[1], Andrea Bevilacqua[1], Antonella Bertagnini[1], Massimo Pompilio[1], Patrizia Landi[1], Paola Del Carlo[1], Alessio Di Roberto[1], and Willy Aspinall[2]

[1]Istituto Nazionale di Geofisica e Vulcanologia
[2]University of Bristol

November 23, 2022

Abstract

The study focuses on the estimation and modeling of the temporal rates of major explosions and paroxysms at Stromboli volcano (also named small-scale and large-scale paroxysms respectively). The analysis was further motivated by the paroxysm of July 3rd 2019, which raised, once again, the attention of the scientific community and civil protection authorities on the volcanic hazards of Stromboli. In fact, at the present state of knowledge, major explosions and paroxysms cannot be forecasted based on monitoring data, and a full probabilistic assessment based on past eruption data would be quite useful for scientific and civil protection purposes. In the study we perform a time series analysis either considering the last ˜150 years of reconstructed activity and the most recent 35 years. We included the estimation of event rates and rate changes in time. Results clearly highlight that the activity is non-homogeneus in time, with a significant low of activity between about 1960 and 1990. Maximum values of event rates were computed during the first half of last century, for both major explosions and paroxysms, whereas the rate of paroxysms is significantly lower in the last decades with respect to maximum rates. We also accomplish a statistical analysis of the inter-event times, enabling us to determine if the data can be modeled as a Poisson process or not, e.g. if it shows time dependent distributions, recurring cycles, or temporal clusters. The uncertainty quantification on the current and future rates is mainly related to the choice of the modeling assumptions. The study represents a crucial progress towards quantitative hazard and risk assessments at Stromboli, which is particularly relevant for the thousands of people (e.g. tourists, guides and volcanologists) that regularly climb the volcano every year.

Temporal rates of major explosions and paroxysms at Stromboli: data and statistical models

Augusto Neri[(1)], **Andrea Bevilacqua**[(1)], Antonella Bertagnini[(1)], Massimo Pompilio[(1)], Patrizia Landi[(1)], Paola Del Carlo[(1)], Alessio Di Roberto[(1)], Willy Aspinall[(2)]

(1) Istituto Nazionale di Geofisica e Vulcanologia, Sezione di Pisa, Pisa, Italy, (2) University of Bristol, School of Earth Sciences, Bristol, United Kingdom.

ISTITUTO NAZIONALE DI GEOFISICA E VULCANOLOGIA

AGU 100 ADVANCING EARTH AND SPACE SCIENCE | FALL MEETING | San Francisco, CA | 9–13 December 2019

Paper Number V23I - 0307
Abstract ID: 619672

1. Major explosions and paroxysms datasets and temporal rates

The study focuses on the estimation and modeling of the **temporal rates of major explosions and paroxysms at Stromboli volcano** (Italy). See **Tab. 1** for definitions, **Fig. 2, 8** for some pictures. Since, at the present state of knowledge, major explosions and paroxysms cannot be forecasted based on monitoring data, a probabilistic assessment using past eruption data is useful and informative for **scientific and civil protection purposes**. Results allow to quantify the probability of occurrence of these phenomena and highlight that the explosive activity is strongly non-homogeneous in time. Maximum values of event rates for both major explosions and paroxysms were computed during the **first half of last century**, whereas the rate of paroxysms in the last decades of the century has been **significantly decreased** (see **Fig. 3**). The study is a further step towards quantitative hazard and risk assessments at Stromboli, which are particularly relevant for the thousands of people (e.g. **tourists, guides and volcanologists**) that climb the volcano every year.

We performed a statistical analysis of the **historical record** of major explosions and paroxysms at Stromboli, by using the datasets in Barberi et al., (1993), Rosi et al., (2013), and INGV weekly bulletins, with a few changes after a new analysis of the original documents.

We developed three types of models:
1) **Non-homogeneous Poisson models** based on the annual rates over various time windows of T = 2, 5, 10, or 25 years (**Fig. 3, 7**).

2) **Non-parametric models** directly describing the observed inter-event time (**Fig. 4, 7**), and a simple analysis of the clusters of events (**Tab. 2**).

3) **Markov models** using maximum likelihood functions for the inter-event time, considering Weibull and lognormal classes (**Fig. 6, 10**).

	NORMAL ACTIVITY	MAJOR EXPLOSIONS	PAROXYSMS
Total duration	4–30 s	<2 min	*c.* 5–10 min
Fall-out volume	1–10 m^3	10^2–10^3 m^3	10^4–10^5 m^3
Mass Discharge Rate	10^2–10^3 kg/sec	10^4–10^5 kg/s	10^6–10^7 kg/s
Ballistic size	Centimetric	Up to decimetric	Up to metric
Ballistic range	200–250 m	1 km (400 m a.s.l.)	Entire island
Column height	*c.* 50–400 m	*c.* 1000 m	3000–4000 m

Figure 1. Historical representation of the «Semaforo di Labronzo» (Labronzo Lighthouse).

Table 1. Comparison of the main parameters for normal activity, major explosions and paroxysms (from Rosi et al., 2013).

The latter include data available from 1930, 2003 and 2007 events (Rosi et al. 2006; Bertagnini et al. 2011; Pistolesi et al. 2011).

Ballistic size is intended as the diameter of material at the maximum distance from the vent (ballistic range).

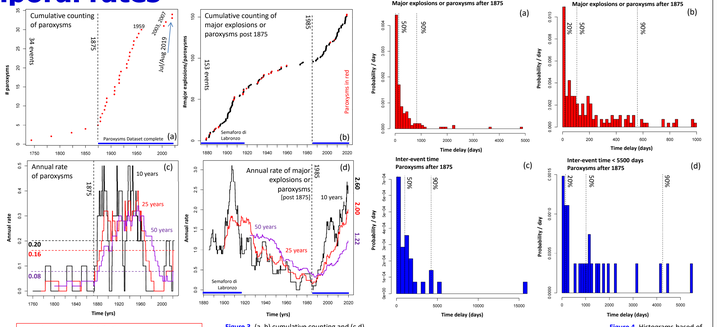

Figure 3. (a, b) cumulative counting and (c,d) annual rate of major explosions or paroxysms. (a, c) only consider the paroxysms. The current annual rate is displayed. Time intervals with improved completeness of the dataset are marked in blue.

A non-homogeneous distribution:
(i) with **undercrecording effects** (e.g. before 1875)
(ii) with **annual rate changes** (e.g. in 1960 and 1985)

Figure 4. Histograms based of the inter-event time of (a,b) major explosions or paroxysms, and (c,d) only paroxysms.

We consider all the pairs of consecutive events observed after 1875.

This statistics describes the entire dataset post 1875, and not only the current annual rate.

Figure 2. Examples of paroxysms, (a,b) Nov 13, 1915, (c,d) Jul 11, 1959, (e,f) Apr 5, 2003, (g,h) Jul 3, 2019, (i) Aug 28, 2019. Modified from Perret, (1916), Cavallaro, (1962), Rosi et al., (2006); INGV bulletins.

In (L) we show an aerial overview of the island taken in 1960. Modified from Cavallaro (1962).

Time intervals with improved completeness of the dataset of major explosions:
1874-1916 [Semaforo di Labronzo, Fig. 1]
1985-2019 [frequent scientific observations]

The dataset of paroxysms is very likely to be 100% complete after 1875.

The annual rate is based on left-side first order finite differences:

$$\lambda(t) = \frac{N(t) - N(t - T)}{T}$$

The annual rate is based on the left-side interval so that the value at time t is not anticipating future information which is unvailable at time t.

Non-parametric model directly describing the data

(a) inter-event time of major explosions or paroxysms	(b) inter-event time of paroxysms
5% probability < 4.1 days	5% probability < 46.2 days
20% < 19.4 days	20% < 5 months
50% < 5 months	50% < 2.8 years
90% < 27 months	90% < 11.5 years

2. Models of inter-event time based on maximum likelihood functions

2 triplets
6 pairs
12 single

PAROXYSMS
1879 2 5
123 days
1879 6 8

1891 6 24
68 days
1891 8 31

1906 7 11
184 days
1907 1 11
106 days
1907 4 27

1915 11 13
13 days
1915 11 26
219 days
1916 7 3

1930 9 11
41 days
1930 10 22

1936 1 31
268 days
1936 10 26

1943 12 3
260 days
1944 8 20

2019 7 3
56 days
2019 8 28 (a)

MAJOR EXPLOSIONS
1879 2 4
1 days
1879 2 5

1898 10 20
5 days
1898 10 25

1900 7 19
16 days
1900 8 4
18 days
1900 8 22

1903 3 9
5 days
1903 3 14
11 days
1903 3 25
3 days
1903 3 28

1905 2 25
18 days
1905 3 15
2 days
1905 3 17

1907 1 11
16 days
1907 1 27

1907 4 13
14 days
1907 4 27

1915 11 13
13 days
1915 11 26

1916 6 20
12 days
1916 7 2
1 day
1916 7 3
1 day
1916 7 4

1921 6 4
12 days
1921 6 16
6 days
1921 6 22

1954 1 30
2 days
1954 2 1

1996 6 1
5 days
1996 6 6

1998 8 23
16 days
1998 9 8

1998 12 26
2 days
1998 12 28

2009 11 8
16 days
2009 11 24

3 quartets
5 triplets
15 pairs
96 single

2010 1 10
11 days
2010 1 21

2011 7 5
5 days
2011 7 10
7 days
2011 7 17
19 days
2011 8 5

2013 12 4
21 days
2013 12 25
10 days
2014 1 4

2017 10 23
9 days
2017 11 1

2018 3 7
11 days
2018 3 18

2018 4 24
2 days
2018 4 26

2019 6 25
8 days
2019 7 3 (b)

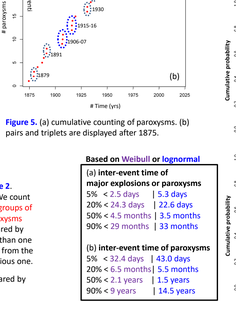

Figure 5. (a) cumulative counting of paroxysms. (b) pairs and triplets are displayed after 1875.

Table 2.
(a) We count the **groups of paroxysms** separed by less than one year from the previous one.

(b) We counted the groups of major explosions or paroxysms separed by less than one month from the previous one.

Based on Weibull or lognormal

(a) **inter-event time of major explosions or paroxysms**

5% < 2.5 days	5.3 days
20% < 24.3 days	22.6 days
50% < 4.5 months	3.5 months
90% < 29 months	33 months

(b) **inter-event time of paroxysms**

5% < 32.4 days	43.0 days
20% < 6.5 months	5.5 months
50% < 2.1 years	1.5 years
90% < 9 years	14.5 years

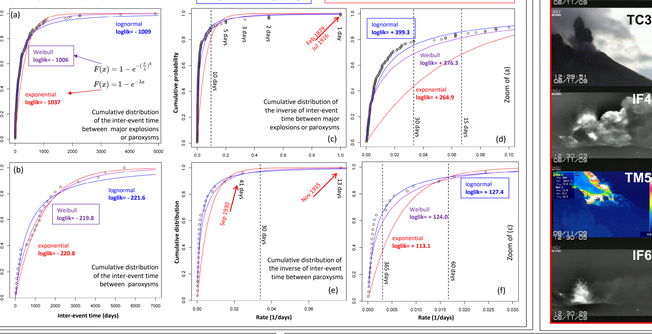

Figure 6. Cumulative distribution functions of the maximum likelihood fit of (a, b) the inter-event time between major explosions or paroxysms and (c, e) their inverse. (d, f) zoom on the shortest times. (b, e) only consider the paroxysms.

Lognormal function fits on the inter-event time and their inverse are equal, because of symmetry.

A **Weibull** function can be half-way between an exponential and a lognormal. It is the class that best approximates the inter-event times at Stromboli. The **lognormal** class shows the best performance in the modeling of the inverse of the inter-event time.

Radial range of ballistic bombs

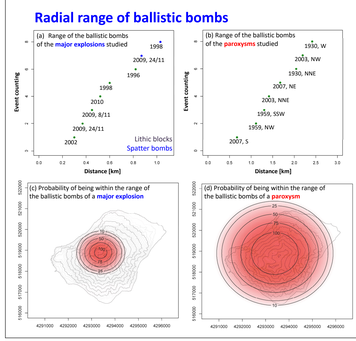

Figure 13. (a, b) **maximum range** reached by ballistic bombs (a) of major explosions in 1996, 1998, 2002, 2009, 2010, and (b) the paroxysms in 1930, 1959, 2003 e 2007.

(c, d) **probability maps** of being within the range of ballistic bombs of (c) major explosions, and (d) paroxysms.

Reported values are probability percentages.

To be considered as hazard maps, the estimates on the left lack of:

1) estimates of the **angular amplitude**, possibly less than a round-angle, interested by the bombs.

2) **possible preferential directions** of the bombs.

3) The probability of being in a section reached by the bombs, but **not hit**. (*spatial density of the impacts*).

Radial directions of ballistic bombs

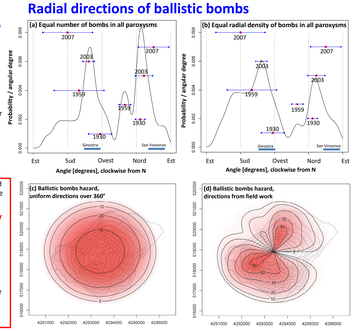

Figure 14. (a,b) Probability density functions of the **directions** of the ballistic bombs of the paroxysms in 1930, 1959, 2003 e 2007. Reported values are probabilities over degrees.

In (a) we assume an **equal number** of bombs inside every sector interested by a paroxysm. Peaks of probability are observed in the directions SW and NNE.

In (b) we assume a uniform and **equal angular density** of the bombs inside every sector interested.

(c, d) **hazard maps** of ballistic bombs. (c) assumes a **uniformly distributed direction** over a round-angle, and (d) a direction weighted **according to (b)**.

Reported values are the probability **percentages** to be reached by the bombs.

Both maps assume an angular amplitude equal to the **average** of the historically observed angles: [75°, 85°, 160°, 210°].

Figure 12. Examples of metric-scale ballistic bombs produced during paroxysms of (a) Jul 11, 1959, (b-c) Apr 5, 2003, (d) Mar 15, 2007, (e-f) Jul 3, 2019. Modified from Cavallaro (1959), Rosi et al., (2013), INGV (2019a).

Figure 11. Examples of maps describing the effects of paroxysms in (a) Sep 11, 1930 and (b) Apr 5, 2003, and Mar 15, 2007.

Modified from Rosi et al., 2013, and Bertagnini et al., 2008, with an original Table from Rittmann, 1931.

3. Major explosions and paroxysms post 1985 and in 1875-1916

Figure 7. (a, d) cumulative counting and (b, e) histograms of inter-event time, and (c, f) annual rate, of major explosions or paroxysms post 1985 and in 1875-1916.

In both the subdatasets we observe a higher annual rate than in the dataset post 1875.

The dataset in 1875-1916 is similar to the dataset post 1985. We observe an even higher annual rate but a long gap in 1907-1912.

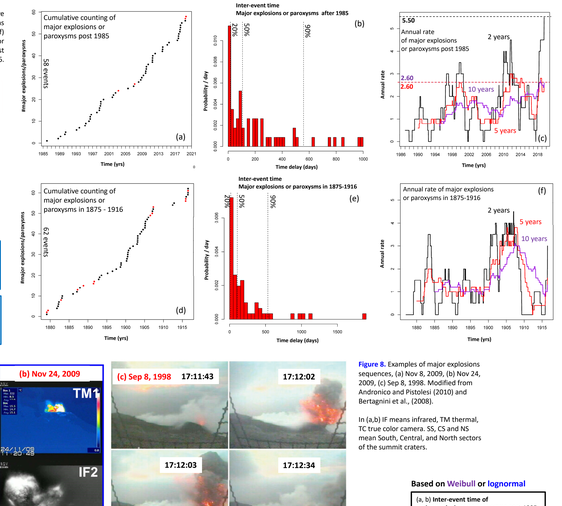

Non-parametric model directly describing the data

inter-event time of major explosions or paroxysms

Based on data post 1985
5% probability < 5.0 days
20% < 16.6 days
50% < 3 months
90% < 18 months

Based on data in 1875-1916
5% probability < 2.0 days
20% < 16.0 days
50% < 3 months
90% < 17.5 months

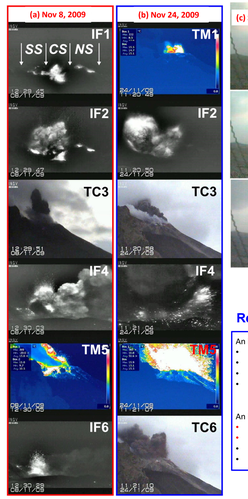

Figure 8. Examples of major explosions sequences, (a) Nov 8, 2009, (b) Nov 24, 2009, (c) Sep 8, 1998. Modified from Andronico and Pistolesi (2010) and Bertagnini et al., (2008).

In (a,b) IF means infrared, TM thermal, TC true color camera. SS, CS and NS mean South, Central, and North sectors of the summit craters.

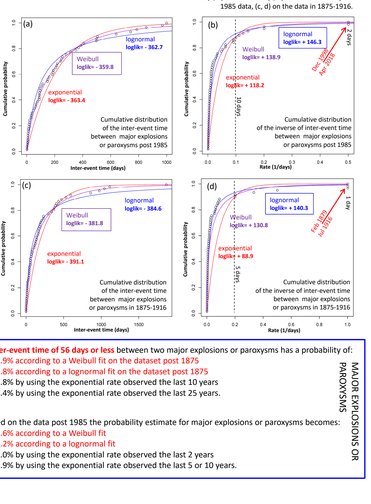

Figure 9. Recent photos of (a,d) Sciara del Fuoco, and (b,c) Pizzo, showing the island features.

Figure 10. Cumulative distribution functions of the maximum likelihood fit of (a, c) the inter-event time between major explosions or paroxysms and (b, d) their inverse. (a, b) are based on the post 1985 data, (c, d) on the data in 1875-1916.

Based on Weibull or lognormal

(a, b) **Inter-event time of major explosions or paroxysms post 1985**
5% probability < 3.9 days | 6.1 days
20% < 26.6 days | 22.3 days
50% < 4 months | 3 months
90% < 18 months | 22.5 months

(c, d) **Inter-event time of major explosions or paroxysmin 1875-1916**
5% probability < 2.1 days | 3.9 days
20% < 19.0 days | 16.3 days
50% < 3.5 months | 2.5 months
90% < 19.5 months | 24 months

Violet adopts a Weibull function
Blue adopts a lognormal function

Retrospective probability estimates

An **inter-event time of 15974 days or more**, i.e. ~43.7 years, between two paroxysms has a probability of:
- 0.025% (i.e. 2.5 x 10^{-4}) according to a Weibull fit on the dataset post 1875
- 2.5% according to a lognormal fit on the dataset post 1875
- 0.016% (i.e. 1.6 x 10^{-4}) by using the exponential rate observed the last 10 years
- 0.091% (i.e. 9.1 x 10^{-4}) by using the exponential rate observed the last 25 years

a lognormal has a better performance than the other functions
In the modeling of inverse inter-event times

An **inter-event time of 56 days or less** between two paroxysms has a probability of:
- **7.7%** according to a Weibull fit on the dataset post 1875
- **6.9%** according to a lognormal fit on the dataset post 1875
- 3.0% by using the exponential rate observed the last 10 years
- 2.4% by using the exponential rate observed the last 25 years.

MAJOR EXPLOSIONS OR PAROXYSMS

An **inter-event time of 56 days or less** between two major explosions or paroxysms has a probability of:
- **31.9%** according to a Weibull fit on the dataset post 1875
- **36.8%** according to a lognormal fit on the dataset post 1875
- 32.8% by using the exponential rate observed the last 10 years
- 26.4% by using the exponential rate observed the last 25 years.

If based on the data post 1985 the probability estimate for major explosions or paroxysms becomes:
- **32.6%** according to a Weibull fit
- **39.2%** according to a lognormal fit
- 57.0% by using the exponential rate observed the last 2 years
- 32.9% by using the exponential rate observed the last 5 or 10 years.

4. Preliminary hazard mapping of ballistic bombs

On the basis of a critical review of field data related to the dispersal area of **ballistic bombs** from major explosions and paroxysms occurred at Stromboli (see **Fig. 11, 12**), we propose a probabilistic hazard map of the areas exposed to future events.

First, a **conditional probability map**, i.e. under the assumption of having a major explosion or a paroxysm, is calculated on the base of a Monte Carlo simulation varying circular sectors exposed to the bombs (**Fig. 13**). The sectors are assumed to have an uncertain **radial range, direction, and angular amplitude**. Due to the limited number of explosions that are well-mapped, and to a possible under-recording of the bombs distribution in some parts of the island, we also perform a sensitivity analysis assuming uniform directions and a round-angle exposed area.

Then, we combine the temporal model of major explosions and paroxysms with these estimates. The result is a map of the **absolute annual probability of being exposed** to ballistic bombs (**Fig. 14**).

5. Towards quantitative risk assessments

The spatio-temporal probability maps can also be used to provide **first quantitative estimates of the risk rates** taken by guides, volcanologists, tourists and people living on the island year-long. The total time that each person spends inside the areas exposed to the bombs, over a year, defines the **annual risk taken** by the **individual**. We show that, depending on the memory properties of the temporal models, the **risk levels are not constant** and they can increase for some weeks after any explosive event, if compared with their mean statistics (**Fig. 15**).

Example of cumulative risk and equivalent time

On the base of the annual rates of major explosions and paroxysms, it is possible to quantify an order of magnitude for the duration of a **tolerable exposure time** for the subjects that climb to the **summit of the volcano** (e.g. tourists, guides, volcanologists).

This estimate assumes two main simplifying hypotheses, which can both be relaxed after specific analyses:

1) the vulnerability of the exposed subjects is assumed equal to one, i.e. we assume that an event is lethal for any subject exposed to it.

2) the exposure is only determined by the time length, i.e. we assume that the spatial component is not affecting the risk level.

Typically, the **annual tolerable risk** from natural sources is 10^{-3} for workers and 10^{-4} for a general people (like tourists).

We obtain this example of the **total equivalent time** tolerable over one year for an individual:

Example: we assume a constant annual rate of major explosions of 3 events/year:

Tolerable risk = 10^{-4} (general people): 18 minutes
Tolerable risk = 10^{-3} (workers): 3 hours

Statistical models of cumulative risk and equivalent time

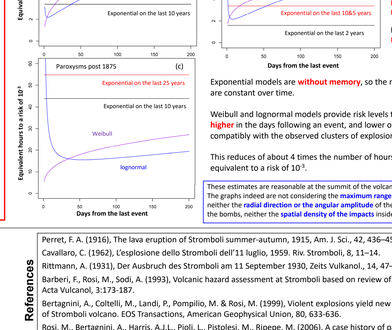

Figure 15. Number of hours **equivalent** to a risk level of 10^{-3}, as obtained from time dependent hazard rates.

(a, b) consider the major explosions and the paroxysms.

(a) is based on the data post 1875, (b) on the data post 1985.

(c) only considers the paroxysms post 1875.

Exponential models are **without memory**, so the risk rates are constant over time.

Weibull and lognormal models provide risk levels that **can be higher** in the days following an event, and lower otherwise, compatibly with the observed clusters of explosions.

This reduces of about 4 times the number of hours equivalent to a risk of 10^{-3}.

These estimates are reasonable at the summit of the volcano.
The graphs indeed are not considering the **maximum range** of ballistic bombs, neither the **radial direction or the angular amplitude** of the sectors interested by the bombs, neither the **spatial density of the impacts** inside the sector.

6. Conclusions

- If we consider the major explosions and the paroxysms as a single class (**Fig. 3**), the annual rate observed in the last 10 years, 2.6 events/year, is close to the maximum observed in the first two decades of 1900, i.e. 3.1 events/year.
- If we consider only the paroxysms (**Fig. 3**), the annual rate observed in the last 10 years, 0.2 events/year, is about half of the maximum registered in the first decades of 1900, i.e. events/year.
- There is a 20% probability that a major explosion or a paroxysm follows the previous after less than 19.4 days (Fig. 4). Based on the data post 1985, this estimate decreases to 16.6 days (**Fig. 7**).
- If we consider the record post 1985 (**Fig. 7**), the inter-event time distribution of major explosions or paroxysms is similar to what observed in 1875-1916, except for a lower chance of events very close in time.
- Based on the data post 1875 there is a 20% probability that a paroxysm follows the previous in less than:
  5 months based on the percentiles of data post 1875 (**Fig. 4**)
  6.5 months according to a Weibull function of maximum likelihood (**Fig. 6**)
  5.5 months according to a lognormal function of maximum likelihood (**Fig. 6**)
- The probability of two paroxysms in less than 56 days (like the time interval 3 Jul-28 Aug) is about 8%.
- The probability of having 44 years without any paroxysm (1959-2003) is of the order of 10^{-4}/10^{-2}.
- After 1875 there were 30 paroxysms, 12 as single events, 6 times as pairs, and 2 times as triples (**Tab. 2, Fig. 5**) (assuming a separation threshold of one year).
- The probabilistic hazard estimates for ballistic bombs during paroxysms, including radial range, angular amplitude of the exposed sector, and possible directionality, describe values above 20% in low elevation zones (**Fig. 13, 14**).
- Apparent hazard peaks in the directions of Ginostra Village and Punta Labronzo might be due to the structure of the craters, but only four paroxysms are currently well-mapped in literature.
  A future analysis including the events in 2019 may further support these preferential directions.
  Assuming uniform directions produces similar hazard levels (**Fig. 14**).
- On an annual basis, illustrative total at-risk times that are tolerable for visits to the crater are 3 hours for workers, and 18 minutes for tourists (tolerable risk for volcanologists may allow longer visits). Risk levels are likely to be elevated in the days and weeks following a major explosion or paroxysm (**Fig. 15**), and perhaps lower at other times.

References

Bertagnini, A., Metrich, N., Francalanci, L., Landi, P., Tommasini, S., Conticelli, S. (2008), Volcanology and magma geochemistry of the present-day activity: constraints on the feeding system. In: AGU, Geophysical Monograph 182, Washington, DC, pp 19-38.

Pistolesi, M., Rosi, M., Pioli, L., Renzulli, A., Bertagnini, A. & Andronico, D. (2008), The paroxysmal event and its deposits. In: AGU, Geophysical Monograph 182, Washington, DC, pp 182, 317–330.

Andronico, D., Pistolesi, M. (2010), The November 2009 paroxysmal explosions at Stromboli. JVGR, 196:120-125.

Bertagnini, A., Di Roberto, A., Pompilio, M. (2011), Paroxysmal activity at Stromboli: lessons from the past. Bull Volcanol, 73, 9, 1229-1243.

Pistolesi, M., Delle Donne, D., Pioli, L., Rosi, M. & Ripepe, M. (2011), The 15 March 2007 explosive crisis at Stromboli volcano, Italy: assessing physical parameters through a multidisciplinary approach. JGR, 116, B12206.

Rosi, M., Pistolesi, M., Bertagnini, A., Landi, P., Pompilio, M., Di Roberto, A. (2013), Stromboli volcano, Aeolian Islands (Italy): present eruptive activity and hazards. In: Geol Soc Lon Mem 37:475–492.

Andronico, D., Taddeucci, J., Cristaldi, A., Miraglia, L., Scarlato, P., Gaeta, M. (2013), The 15 March 2007 paroxysm of Stromboli: video-image analysis, and textural and compositional features of the erupted deposit. Bull Volcanol, 75: 733.

Perret, F. A. (1916), The lava eruption of Stromboli summer-autumn, 1915, Am. J. Sci., 42, 436–457.

Cavallaro, C. (1962), L'esplosione dello Stromboli dell'11 luglio, 1959. Riv. Stromboli, 8, 11–14.

Rittmann, A. (1931), Der Ausbruch des Stromboli am 11 September 1930, Zeits Vulkanol., 14, 47–77.

Barberi, F., Rosi, M., Sodi, A. (1993), Volcanic hazard assessment at Stromboli based on review of historical data. Acta Vulcanol, 3:173-187.

Bertagnini, A., Coltelli, M., Landi, P., Pompilio, M. & Rosi, M. (1999), Violent explosions yield new insights into dynamics of Stromboli volcano. EOS Transactions, American Geophysical Union, 80, 633-636.

Rosi, M., Bertagnini, A., Harris, A.J.L., Pioli, L., Pistolesi, M., Ripepe, M. (2006), A case history of paroxysmal explosion at Stromboli: timing and dynamics of the April 5, 2003 event. Earth Planet Sci Lett 243:594-606.

AGU 100 ADVANCING EARTH AND SPACE SCIENCE | FALL MEETING | San Francisco, CA | 9–13 December 2019